Ionospheric studies using GNSS based techniques over west Africa

O. K. OBROU

October 6, 2022

Université FHB Cocody
Laboratoire des Sciences de la Matière et l'Energie Solaire (LASMES)
African Geophysical Society (AGS)

Table of contents

Introduction

Introduction

The ionosphere is a region of an atmosphere where significant numbers of free thermal electrons and ions are present. All bodies in our solar system that are surrounded by neutral-gas envelope, due either to gravitational attraction (e.g., planets) or some other process such as sublimation (e.g., comets), have an ionosphere. Currently, ionospheres have been observed around all but two of the planets, some moons, and comets. We will talk about only the Earth's ionosphere in this presentation

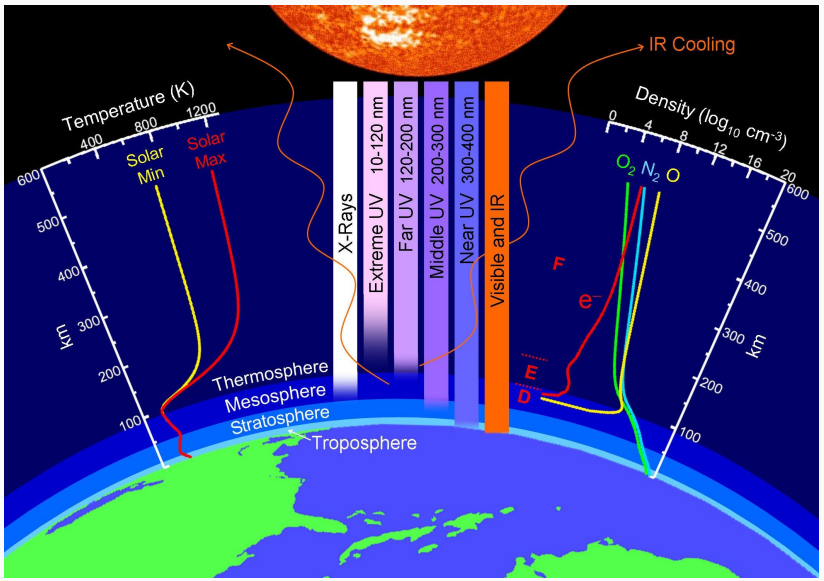

Historical recalls

Historical recalls

1839 : Gauss first speculated that the upper atmosphere might contain ionized regions

Historical recalls

1839 : Gauss first speculated that the upper atmosphere might contain ionized regions

1878 : Stewart postulated the existence of a conductive layer in the upper atmosphere to explain the variations of the Earth's magnetic field observed

Historical recalls

1839 : Gauss first speculated that the upper atmosphere might contain ionized regions

1878 : Stewart postulated the existence of a conductive layer in the upper atmosphere to explain the variations of the Earth's magnetic field observed

1901 : Marconi succeeded in crossing the Atlantic with a radio transmission at a frequency of 300 kHz

Historical recalls

1839 : Gauss first speculated that the upper atmosphere might contain ionized regions

1878 : Stewart postulated the existence of a conductive layer in the upper atmosphere to explain the variations of the Earth's magnetic field observed

1901 : Marconi succeeded in crossing the Atlantic with a radio transmission at a frequency of 300 kHz

1902 : Kennelly & Heaviside both independently suggested that Marconi's signal was propagated by reflection of signals from an ionised layer in the upper atmosphere

Historical recalls

1839 : Gauss first speculated that the upper atmosphere might contain ionized regions

1878 : Stewart postulated the existence of a conductive layer in the upper atmosphere to explain the variations of the Earth's magnetic field observed

1901 : Marconi succeeded in crossing the Atlantic with a radio transmission at a frequency of 300 kHz

1902 : Kennelly & Heaviside both independently suggested that Marconi's signal was propagated by reflection of signals from an ionised layer in the upper atmosphere

1925 : Appleton & Barnett proved the existence of the ionized layer and found its height by doing a phase comparison of two signals from a transmitter, one the ground wave, and the other reflected from the ionosphere

1926 : Breit & Tuve used a pulse technique to measure the heights and critical frequencies of a number of ionospheric layers. Theirs was the first true ionosonde, and may have been the first radar

1926 : Breit & Tuve used a pulse technique to measure the heights and critical frequencies of a number of ionospheric layers. Theirs was the first true ionosonde, and may have been the first radar

1931 : Chapman presented a theory for the formation of an ionized layer due to the action of solar ultraviolet radiation

1926 : Breit & Tuve used a pulse technique to measure the heights and critical frequencies of a number of ionospheric layers. Theirs was the first true ionosonde, and may have been the first radar

1931 : Chapman presented a theory for the formation of an ionized layer due to the action of solar ultraviolet radiation

1932 : Appleton developed an extensive set of equations used to describe the propagation of radio waves in the ionosphere. These included absorption effects and modification due to the Earth's magnetic field

Formation of the Ionosphere

Temperature profile of the Earth's atmosphere

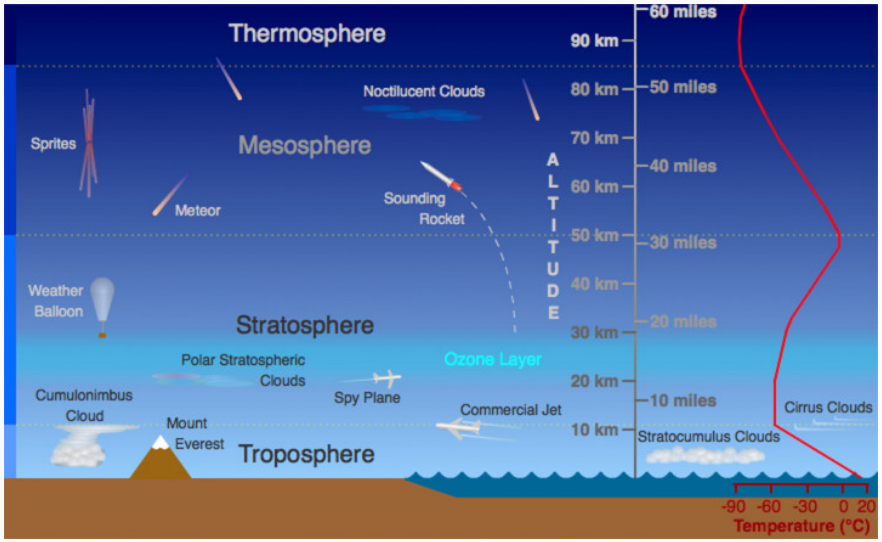

Figure 1: Temperature profile

The atmosphere can be described as a number of layers (-spheres) separated by transition fine layers (-pauses) defined as the inflection points of the temperature profile. This layers are as follow

- The *troposphere* is heated mainly by the ground, which absorbs solar radiation and re-emits it in the infra-red.
- The stratosphere above the troposphere has a positive temperature gradient due to heating from the ozone which absorbs the solar ultra-violet radiation that penetrates down to these altitudes.
- The mesosphere, above 50 km, where the density of ozone drops off faster than the increase of the incoming radiation. The temperature therefore decreases with the altitude.
- The thermosphere is heated mainly by absorption of EUV and XUV radiation through dissociation of molecular oxygen.

Neutral Composition of the Atmosphere

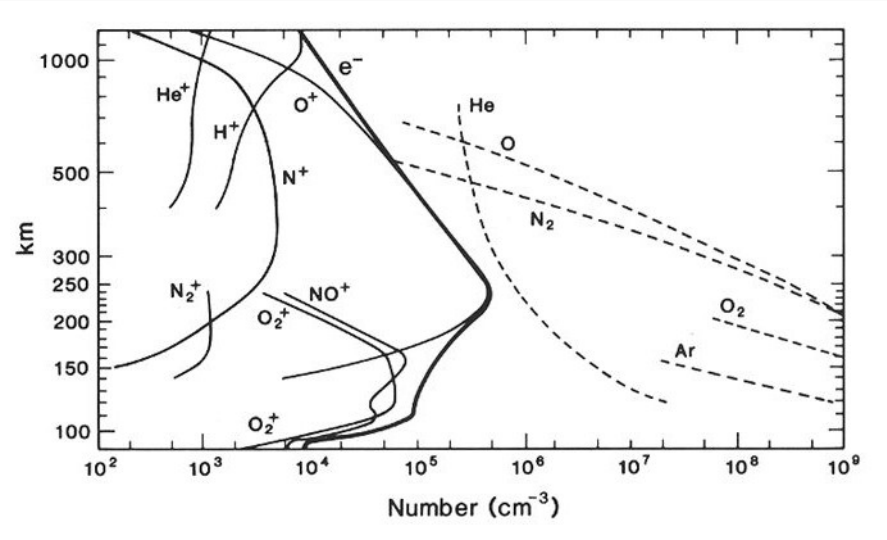

The Earth's atmosphere is made up of a large number of chemical constituents

- Photochemical processes play a fundamental role in the middle and upper atmosphere including the ionosphere
- The density of all constituants decreases with increasing altitude
- N_2, O and He are the most important chemical elements in terms of density

Chemical processes in the upper atmosphere

The ionosphere is formed when extreme ultraviolet light from the sun strips electrons from neutral atoms of the Earth's atmosphere.

Photoionization

When a bundle of EUV light also called photon hits a neutral atom such as oxygen atom, its energy is transferred to an electron in the neutral atom which can then escape from the atom and move freely around. The neutral atom becomes positively charged and is known as a positive ion. The process in which the photon strips an electron from a neutral atom to creat a positive ion is known as Photoionization.

Chemical processes in the upper atmosphere

The ionosphere is formed when extreme ultraviolet light from the sun strips electrons from neutral atoms of the Earth's atmosphere.

Photoionization

When a bundle of EUV light also called photon hits a neutral atom such as oxygen atom, its energy is transferred to an electron in the neutral atom which can then escape from the atom and move freely around. The neutral atom becomes positively charged and is known as a positive ion. The process in which the photon strips an electron from a neutral atom to creat a positive ion is known as Photoionization.

Recombination

The production of free electrons in the ionosphere is balanced by a reverse process. A negatively charged electrons and positively charged ions combined together to produce neutral atoms. This is the main process by which electrons are lost in the ionosphere.

Characteristics of the Ionosphere

Ionospheric layers

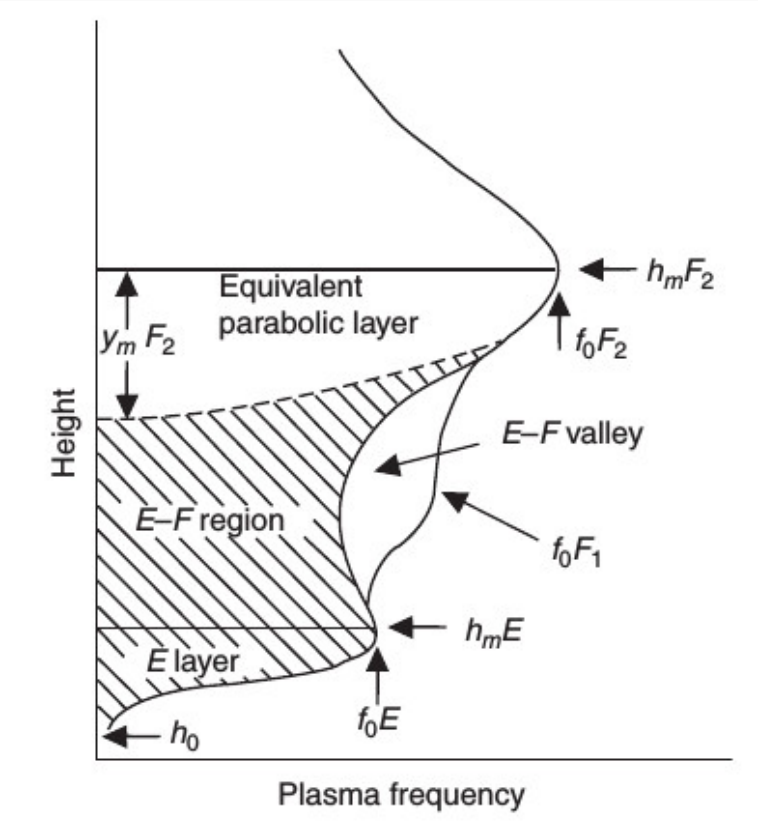

Due to different ionization production and loss processes the electron density profile with altitude shows a layered structure that changes with time, location and solar activity as it is seen in the figure.

- The D region is situated around 90 km with a maximum density of about $1.5 \times 10^4 e/cm^3 (noon)$. Enhanced ionization following solar flares. $\alpha = 3 \times 10^{-8} cm^3/s$
- The E region height is about 110 km with a maximum density of $1.5 \times 10^5 e/cm^3 (noon)$. The production of electron is essentially due to the absorption of EUV ($h\nu > 12eV$) by O_2. The main recombination process is dissociative ($O_2^+ + e^- \rightarrow O + O$) and ($NO^+ + e^- \rightarrow N + O$). $\alpha_D = 1 \times 10^{-8} cm^3/s$

Ionospheric layers cont.

- The F1 region is due to the ionization of O by Lyman "continium" or by emission lines of He. F1 disappers rapidly after sunset. It is located around 200 km with a maximum density of about $2.5 \times 10^5 e/cm^3(noon)$. $\alpha_i = 7 \times 10^{-9} cm^3/s$. O^+ transfer charge to NO
- The F2 region height is above 300 km with a maximum density of $10^6 e/cm^3(noon)$ and $10^5 e/cm^3(night)$. The production of electron is essentially due to ionization of O_2. The main recombination process is radiative with a rate α_R oscillating between 10^{-10} and $10^{-9} cm^3/s$. The height and electron density in the F2 region are highly variable and depends on the day, season and solar sunspot cylce.

The equatorial ionosphere

The equatorial ionosphere

By definition
The equatorial and low latitude ionosphere is the region where the Earth's magnetic field lines are nealy horizontal. At this latitudes the electric field $\overrightarrow{E}_y$ (eastward) is mutually perpendicular to the magnetic field $\overrightarrow{B}$ (northward) and the electron gradient $\overrightarrow{V}_d$ (upward).

The sheet current

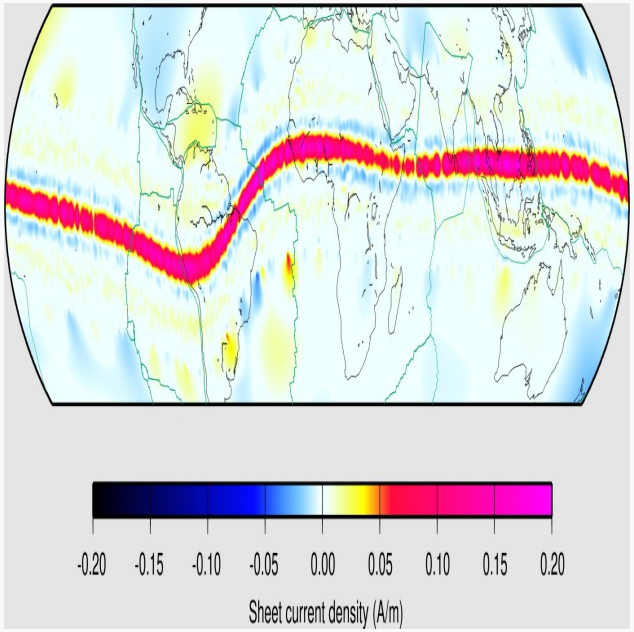

Figure 2: The Current sheet along the magnetic equator

As a consequence of this unique configuration, the equatorial ionosphere is more susceptible to the most important electrodynamic phenomena such as :

As a consequence of this unique configuration, the equatorial ionosphere is more susceptible to the most important electrodynamic phenomena such as :

i) Equatorial Electrojet (EEJ)

As a consequence of this unique configuration, the equatorial ionosphere is more susceptible to the most important electrodynamic phenomena such as :

i) Equatorial Electrojet (EEJ)

ii) Counter Equatorial Electrojet (CEEJ)

As a consequence of this unique configuration, the equatorial ionosphere is more susceptible to the most important electrodynamic phenomena such as :

i) Equatorial Electrojet (EEJ)

ii) Counter Equatorial Electrojet (CEEJ)

iii) Equatorial ionization Anomaly (EIA)

As a consequence of this unique configuration, the equatorial ionosphere is more susceptible to the most important electrodynamic phenomena such as :

i) Equatorial Electrojet (EEJ)

ii) Counter Equatorial Electrojet (CEEJ)

iii) Equatorial ionization Anomaly (EIA)

iv) Equatorial Spread F (ESF)

Equatorial Electrojet

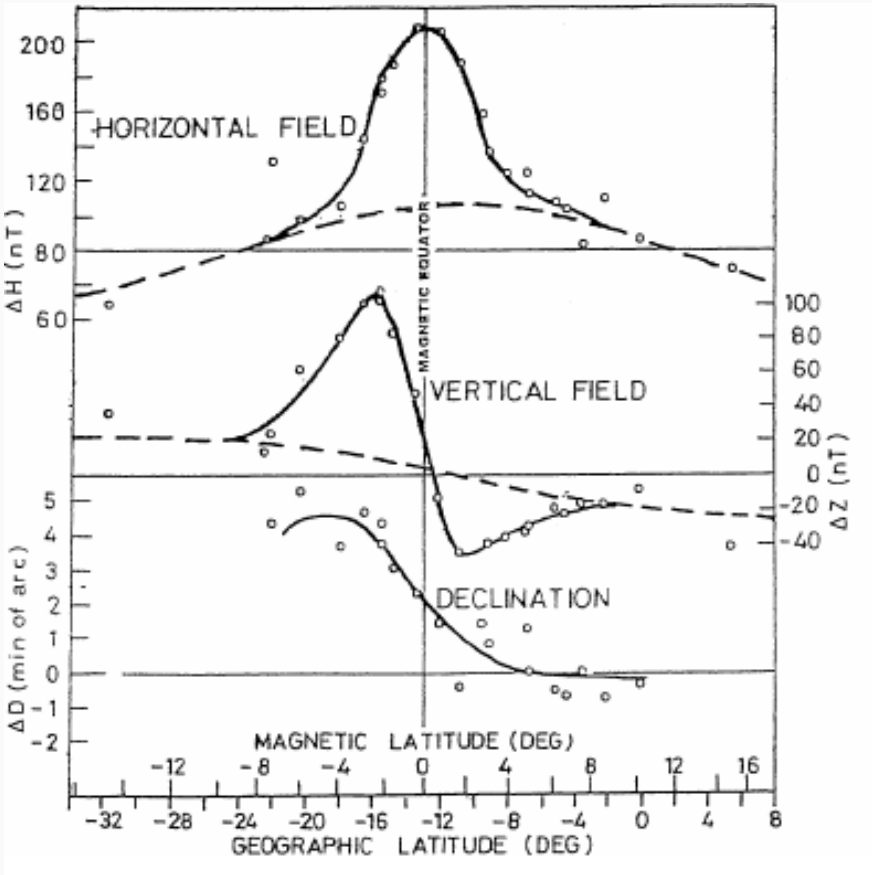

Figure 3: Latitudinal variations of the daily range of H, D and Z along the 75°W meridian during the IGY (Forbush & Casaverde 1961)

1. Chapman (1919) was the first to describe the average S_q variation of the Earth's magnetic components recorded at 21 observatories

Equatorial Electrojet

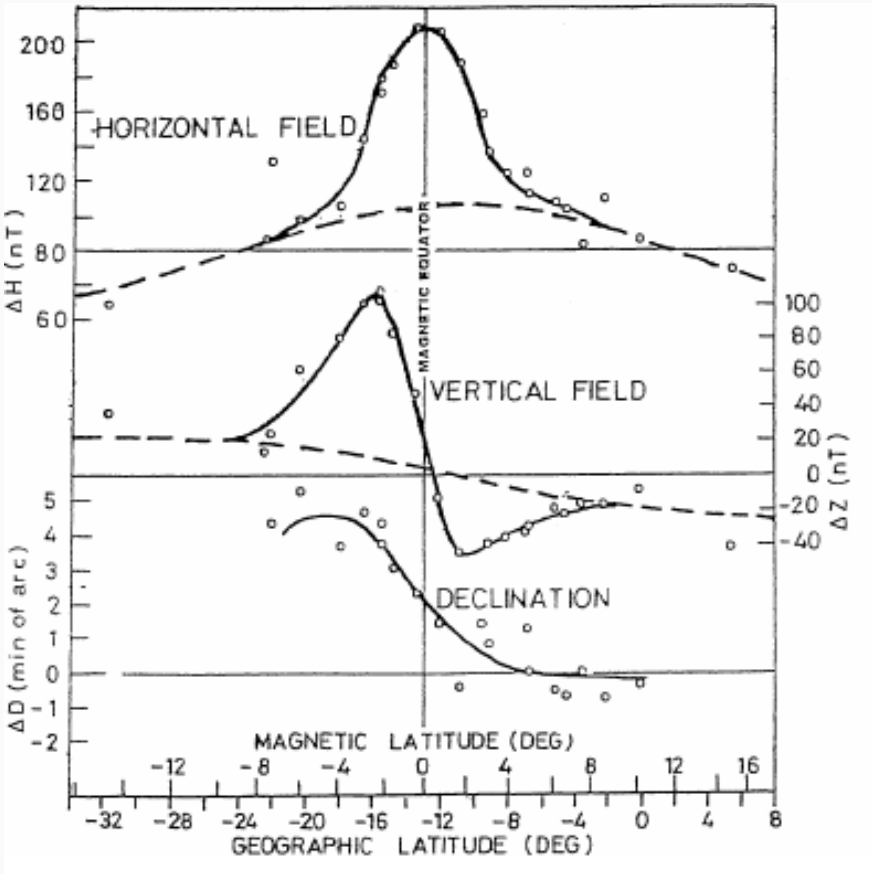

Figure 3: Latitudinal variations of the daily range of H, D and Z along the 75°W meridian during the IGY (Forbush & Casaverde 1961)

1. Chapman (1919) was the first to describe the average S_q variation of the Earth's magnetic components recorded at 21 observatories
2. Egedal (1947) found an abnormal intensification of the daily range of H over the dip equator.

Equatorial Electrojet

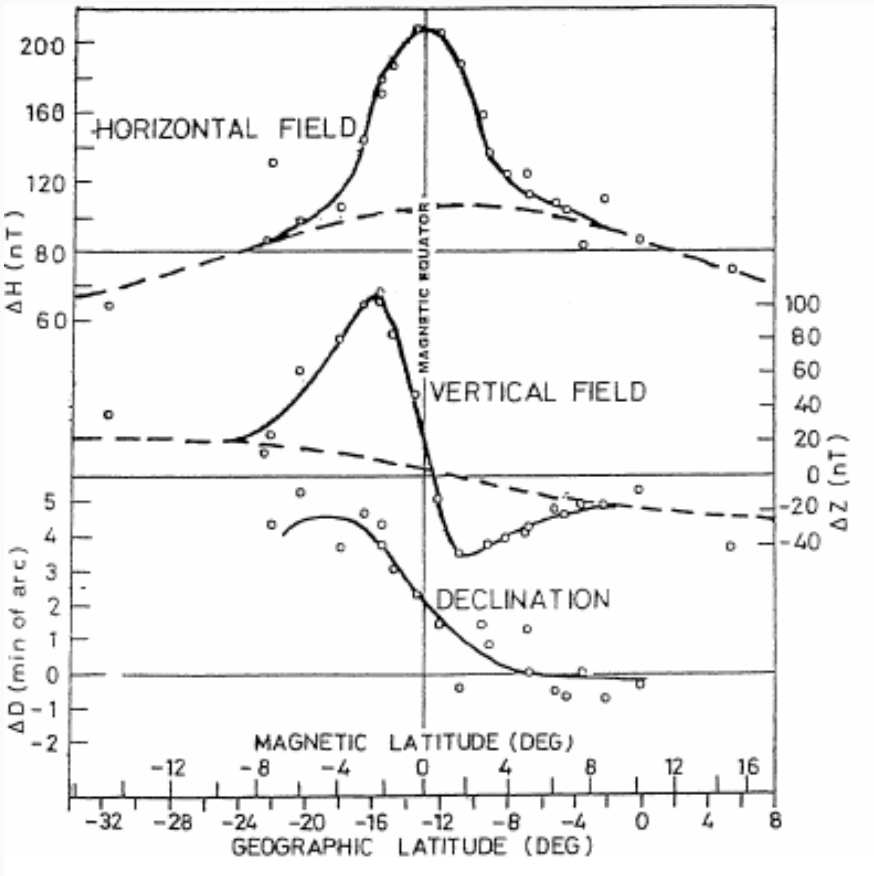

Figure 3: Latitudinal variations of the daily range of H, D and Z along the 75°W meridian during the IGY (Forbush & Casaverde 1961)

1. Chapman (1919) was the first to describe the average S_q variation of the Earth's magnetic components recorded at 21 observatories
2. Egedal (1947) found an abnormal intensification of the daily range of H over the dip equator.
3. This phenomenon was ascribed by Chapman (1951) as due to an eastward band of electric current in the ionosphere, which he named the *'equatorial electrojet'*

- In the E region, the gyrofrequency of the ions Ω_i is almost equal to the collision frequency ν_{in}. The electrons and the ions move at different speeds. It results from this an eastward current.

- In the E region, the gyrofrequency of the ions Ω_i is almost equal to the collision frequency ν_{in}. The electrons and the ions move at different speeds. It results from this an eastward current.
- Above the E region, the gyrofrequencies (Ω_i , Ω_e) are greater than collision frequency (ν_{in}, ν_{en}). The ions and the electrons move at the same speed. No current could be established

- In the E region, the gyrofrequency of the ions Ω_i is almost equal to the collision frequency ν_{in}. The electrons and the ions move at different speeds. It results from this an eastward current.
- Above the E region, the gyrofrequencies (Ω_i , Ω_e) are greater than collision frequency (ν_{in}, ν_{en}). The ions and the electrons move at the same speed. No current could be established

- Below the E region the collision frequency (ν_{in}, ν_{en}) are greater than the gyrofrequency (Ω_i , Ω_e). The electron and the ions are carried by the neutral wind at the same speed. No current is established

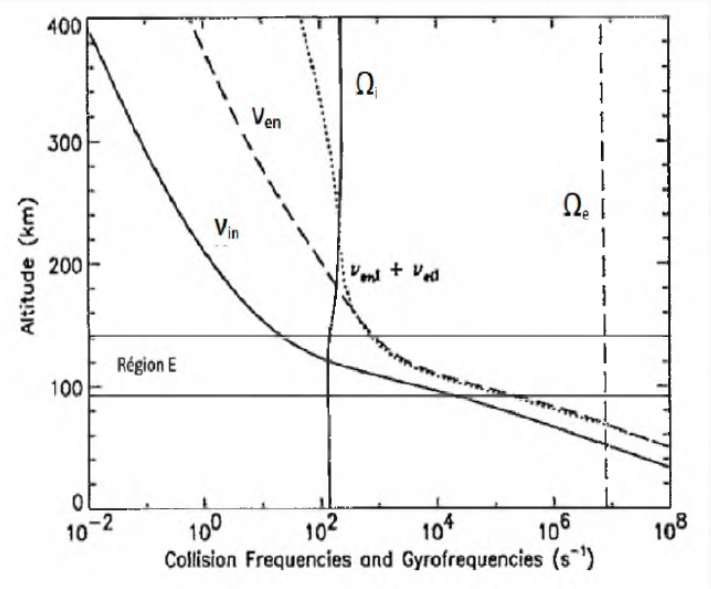

The Basic Equations in 3 steps

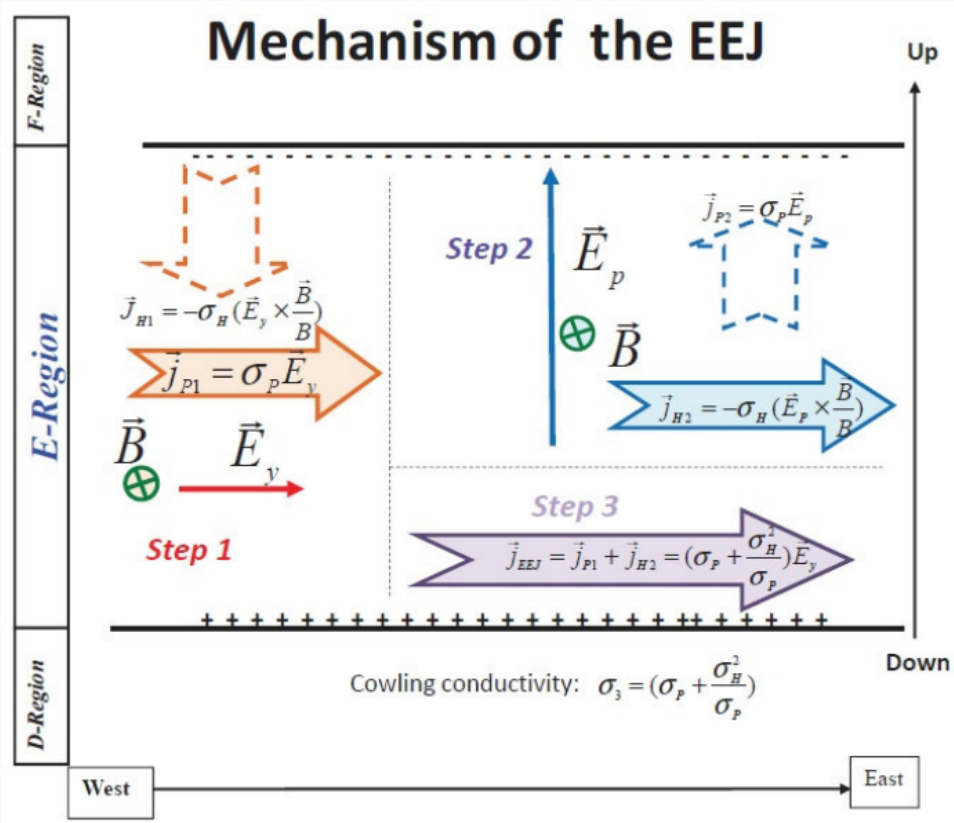

Figure 4: Mecanism of the EEJ(Grodji et al., 2016

The Basic Equations in 3 steps

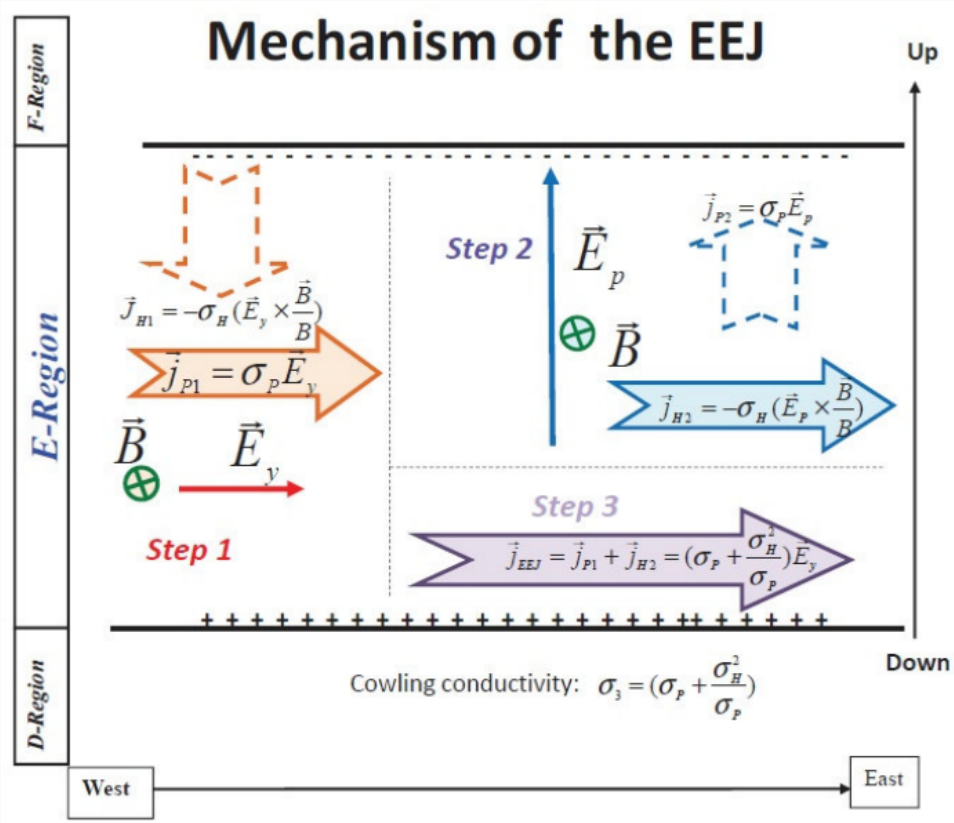

Figure 4: Mecanism of the EEJ(Grodji et al., 2016

- Step 1 : $\overrightarrow{B}$ and the zonal $\overrightarrow{E}_y$ produice an eastward current $\overrightarrow{J}_{p1}$ and a vertical downward Hall current $\overrightarrow{J}_{H1}$

The Basic Equations in 3 steps

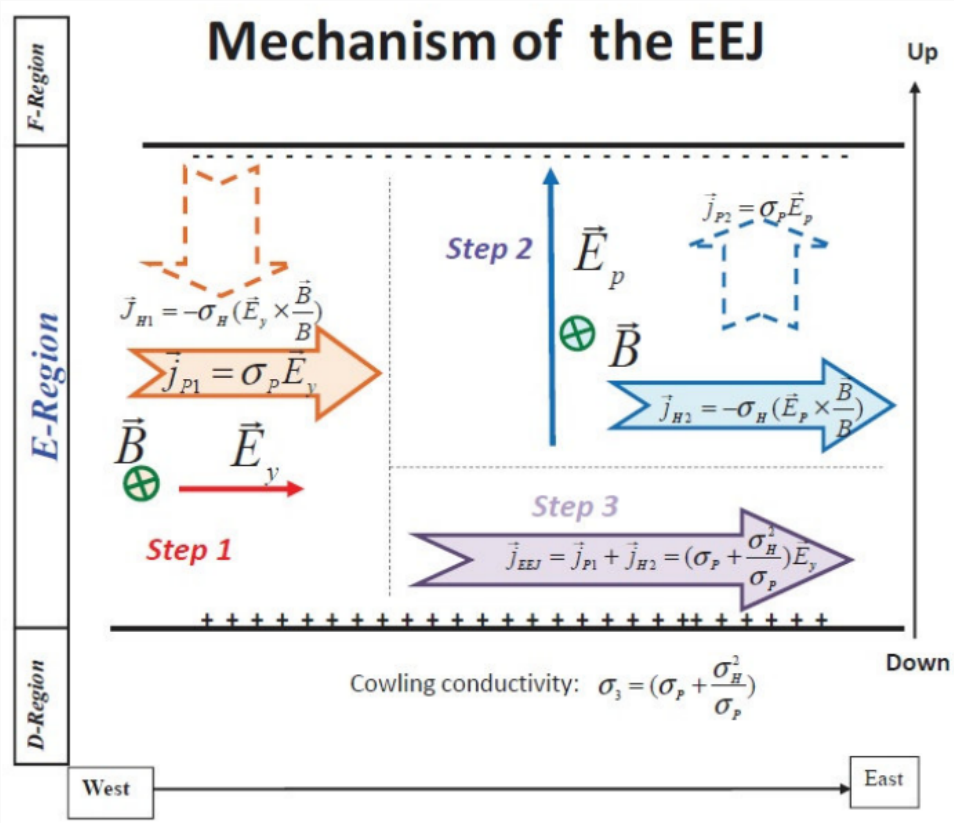

Figure 4: Mecanism of the EEJ(Grodji et al., 2016

- Step 1 : $\overrightarrow{B}$ and the zonal $\overrightarrow{E}_y$ produice an eastward current $\overrightarrow{J}_{p1}$ and a vertical downward Hall current $\overrightarrow{J}_{H1}$
- Step 2 : The ion drift is impeded due to ν_{in}. There is separation of charge that gives rise to an upward electric field $\overrightarrow{E}_p$. The last creats a vertical upward Pedersen current $\overrightarrow{J}_{p2}$. The $\overrightarrow{E}_p \times \overrightarrow{B}$ westward electron drift produce an eastward Hall current

The Basic Equations in 3 steps

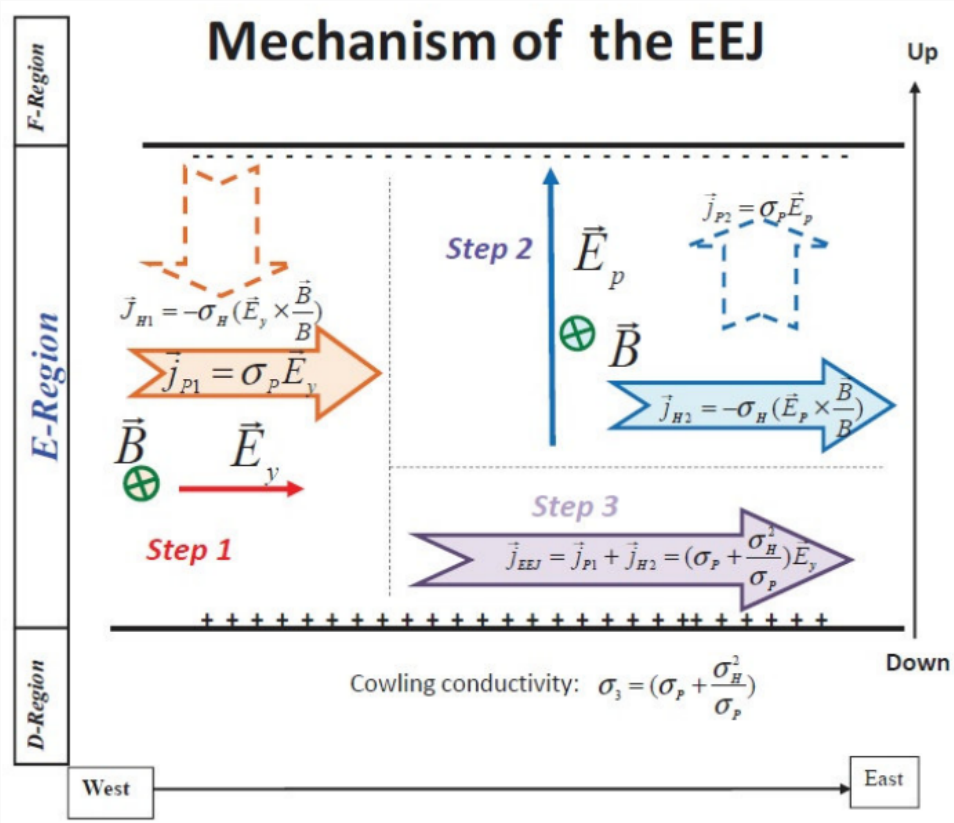

Figure 4: Mecanism of the EEJ(Grodji et al., 2016

- Step 1 : $\overrightarrow{B}$ and the zonal $\overrightarrow{E}_y$ produice an eastward current $\overrightarrow{J}_{p1}$ and a vertical downward Hall current $\overrightarrow{J}_{H1}$
- Step 2 : The ion drift is impeded due to ν_{in}. There is separation of charge that gives rise to an upward electric field $\overrightarrow{E}_p$. The last creats a vertical upward Pedersen current $\overrightarrow{J}_{p2}$. The $\overrightarrow{E}_p \times \overrightarrow{B}$ westward electron drift produce an eastward Hall current
- Step 3 : When the polirization process is complet $\overrightarrow{J}_{H1} + \overrightarrow{J}_{p2} = \overrightarrow{0}$ The total eastward current is

$$\overrightarrow{J}_{EEJ} = \left(\sigma_p + \frac{\sigma_H^2}{\sigma_p}\right) \overrightarrow{E}_y \qquad (1)$$

Observation techniques of the ionosphere

Radio soundings of the ionosphere

The observation of the ionosphere is mainly based on the use of radio wave. Our knowledge of the ionosphere comes from remote sensing by radio waves.

Time of flight
The time of flight is the time delay of a radio wave. There are two methods of measurement

- measurement of the time delay of a pulse
- determination of the stationary phase

Frequency variations
The frequency difference Δf between an echo signal and that of a reference signal is given by

$$\Delta f = -\frac{1}{2\pi}\frac{d\phi}{dt}$$

When the phase ϕ is recorded digitaly Δf can be obtained by numerical differentiation.

Ionosondes

The ionosonde is a sweep-frequency pulsed radar device used to monitor the ionosphere. It frequency can range from below 0.1 MHz to 30 MHz or more with a sweep duration from a few seconds to a few minutes. As the frequency is increased the pulse penetrates to higher levels in the ionosphere. The virtual height increases until the signal penetrates at the critical frequency f_c, which is related to the maximum electron density N_{max} by

$$N_{max} = 1.24 \times 10^{10} f_c^2$$

where N_{max} is in electrons per cubic meter and f_c is in megahertz.

The time delay is obtained by the following equation

$$\Delta t = \frac{2}{c} \int_0^{z(f_p)} \frac{dz}{\mu}$$

where μ is the

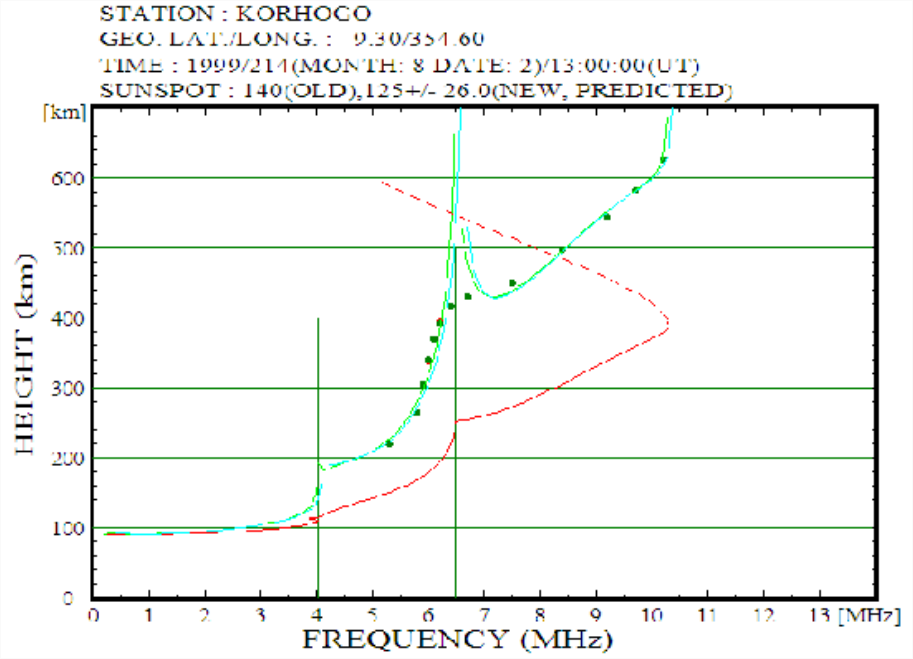

1. On the left we have a scaled ionogram. With the electron density profile in red.
2. On the right an overview of a Kel Aerospace type of ionosonde.

Interpretation of Ionogram

According to the URSI Handbook of ionogram interpretation and reduction edited by W. R. Piggot and K. Rawer, the following tasks are required at any sounding station

- Monitor the ionosphere above the station.
- Obtain significant median data to evaluate long-term changes.
- Study phenomena peculiar to the region.
- Study the global morphology of the ionosphere.

For a simple description of the ionosphere by vertical sounding it is convenient to consider the ionosphere as schematically divided into the conventional regions D, E, F, and the sporadic Es

F Region

$foF2$: critical frequency of the ordinary trace of the highest layer of the F region,called the F2 layer when the F1 layer is present.
fxI : highest frequency recorded by a reflection from the F region.
$foF1$: critical frequency of the ordinary trace of the F1 layer when present.
$h'F2$: minimum virtual height of the ordinary trace of the F2 layer. $h'F$: lowest virtual height of the ordinary trace of the F region.

E Region

foE : critical frequency of the ordinary trace of the E region.

$h'E$:minimum virtual height of the ordinary trace of the E region.

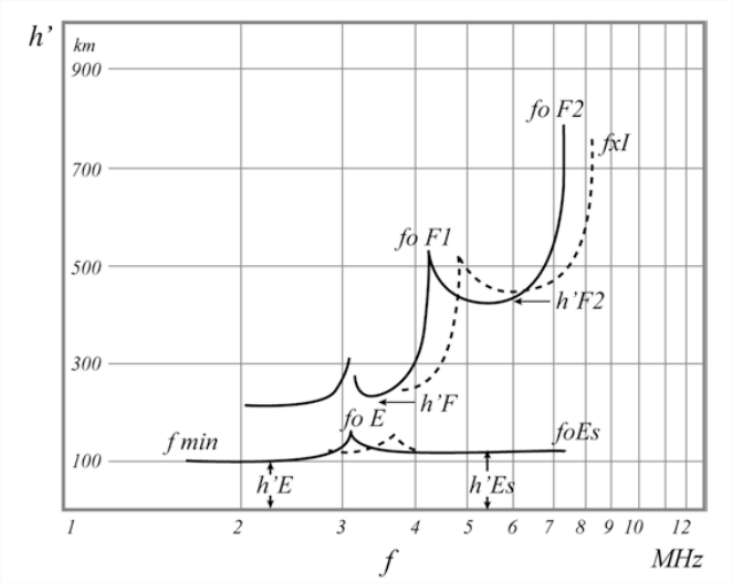

Es Sporadic E layer

foE_s:highest frequency of the ordinary trace of the continuous sporadic E layer.

$h'E_s$:minimum virtual height of the ordinary trace of the Es layer.

f_bE_s :blanketing frequency of the Es layer.

f_{min}:lowest frequency recorded in the ionogram.

Ionospheric data base

The measurements of the principal ionospheric characteristics obtained from scaled ionograms are stored in data based.

1. SPIDR Space Physics Interactive Data Resource:
   `http://spidr.ngdc.noaa.gov/spidr/`
2. ESWUA Electronic Space Weather Upper Atmosphere:
   `http://www.eswua.ingv.it/`
3. DIAS Digital Ionospheric Upper Atmosphere Service:
   `http://www.iono.noa.gr/DIAS/`
4. UMass. Lowell Center for Atmospheric Research:
   `http://umlcar.uml.edu/`

Ionospheric Sounding with GNSS Signals

The refractive index of the ionosphere can be expressed as follows

$$\mu = (1 - X)^{1/2}$$

with

$$X = \frac{\omega_p^2}{\omega^2}$$

where ω_p and ω are respectively the plasma frequency and the frequency of the propagating wave. In fisrt order approximation [1] the phase refractive index is

$$\mu_p \approx 1 - \frac{1}{2}X = 1 - \frac{Ne^2}{2\varepsilon_o m\omega^2}$$

so that

$$\mu_p = 1 - \frac{40.3N}{f^2}$$

and the groupe refractive index is

$$\mu_g = 1 + \frac{40.3N}{f^2}$$

[1] $(1+x)^a = 1 + ax + \frac{a(a-1)}{2}x^2$

Total Electron Content

The total electron content (TEC) is the number of electrons in a column of one metre-squared cross-section along a trans-ionospheric path. It can be obtained by different means, mainly from GNSS and satellite born altimeters signals

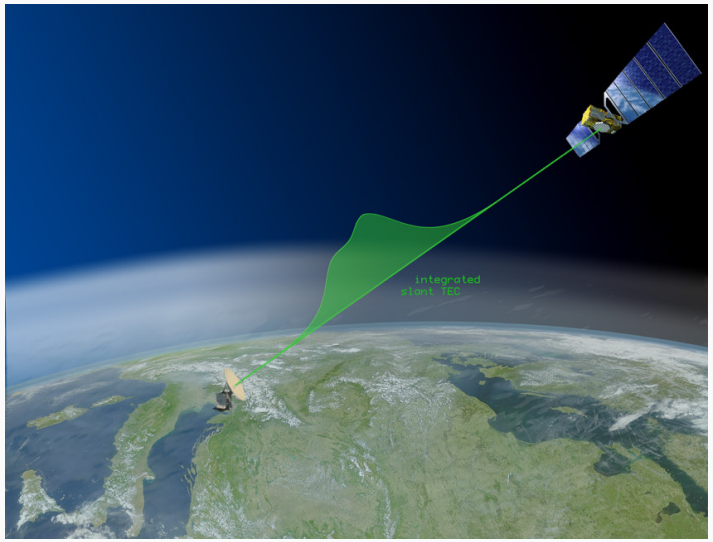

The time delay induced by the phase index is

$$\Delta\tau = \frac{1}{c}\int_u^s (\mu_p(l) - 1)\, dl$$

$$TEC = \int_u^s N(l) dl$$

where N is the electron density of the plasma.
The TEC is expressed in TECU. $1\,TECU = 10^{16}\, el/m^2$

The GNSS infrastructures in west Africa

West African Region's GNSS infrastructures

The West African region is made up of fifteen countries. These countries have both cultural and geopolitical ties and shared common economic interest through the regional organization, the so called ECOWAS.

Figure 5: Map of the members states of ECOWAS

The region is crossed by the magnetic equator. Making it under the influence of the equatorial electrojet and its subsequent effects

The first few IGS stations in the region

Location	Country	Year	Partners
Cotonou	Benin	2008	UNAVCO-JPL/IGN
Dakar	Senegal	2011	CDDIC/DTGC
Toro	Nigeria	2011	UNAVCO-JPL/CGGN
Yakro	Cote d'Ivoire	1999	UNAVCO-JPL/CCT-BNETD

1. CCT-BNETD : Centre de Catographie et de Télédétection
2. CGGN : Center for Geodetic and Geodanymics of Nigeria
3. DTGC : Direction des Travaux Geographiques et Cartographie

Observations

- The raw data are on RINEX Format and freely accessible
- Non of the Universities were involved in the project
- All of the stations were established for the Development of GIS and survey
- The station were established through partnership between National institution and International ones

SAGAIE (Stations ASECNA GNSS pour l'Analyse de la Ionosphère Equatoriale)

Figure 6: SAGAIE Station network (Secretan et al., 2014)

SAGAIE : Stations ASECNA GNSS pour l'Analyse de la Ionosphère Equatoriale (GNSS ASECNA Stations for the Analysis of the Equatorial Ionosphere)

- Implemented by CNES and ASECNA, with the support of Thales Alenia Space
- The stations are all installed at major airports of the region: Dakar, Lomé, Ouagadougou, Douala, and N'Djamena.
- The data are not publicly released

The GNSS stations network in Ivory-Coast

Location	Access	Year	Partners
Abidjan-Cocody	SCINDA	2006	BC/UFHB/CCT-BENETD
Korhogo	Monitor	2017	ESA/UFHB/UGPK
Man	UFHB	2018	UFHB/UMAN
Yakro	IGS	1999	UNAVCO-JPL/CCT-BNETD
Abidjan-Cocody	Not	2014	GLOBEESPACE/CCT-BNETD
Abidjan-Vridi	Not	2015	SEA PORT/CCT-BNETD
Abidjan-Cocody	Not	2018	OXYGEO (PC)
Abidjan-Yopougon	Not	2016	IVOIRTRAVAUX/CCT-BNEDT

The IGS Station is located in Yamoussoukro (Lat : 6.827623, longitude: -5.289343). It was built in 1998 and run under the supersivion of "Bureau National d'Études Techniques et de Développement" Mapping and Remote sensing deparment

The station network in Benin

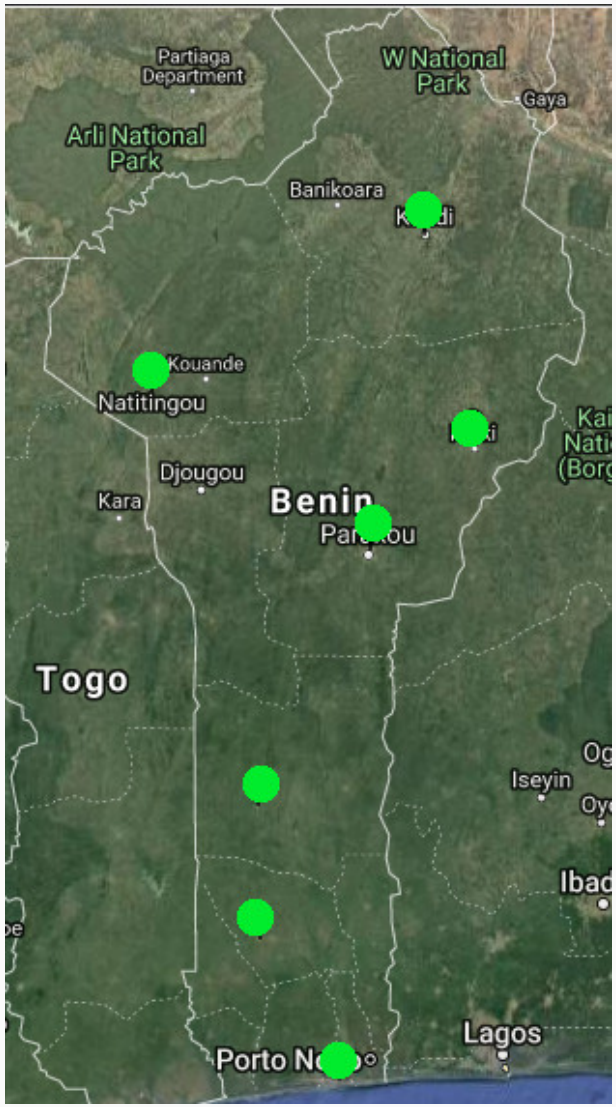

- This network is composed of 7 stations
- Data are stored under RINEX Format
- The data are freely accessible via (`wwww.ign.bj`)
- The network is manage by the Institue Géographique National (IGN) of Benin

The station network in Ghana

- This network is composed of 9 stations
- Data are stored under RINEX Format
- The data are accessible through an authorization
- The network is owned, maintained and operated by Survey and Mapping Division of Ghana Lands Commission.

The station network in Burkina Faso

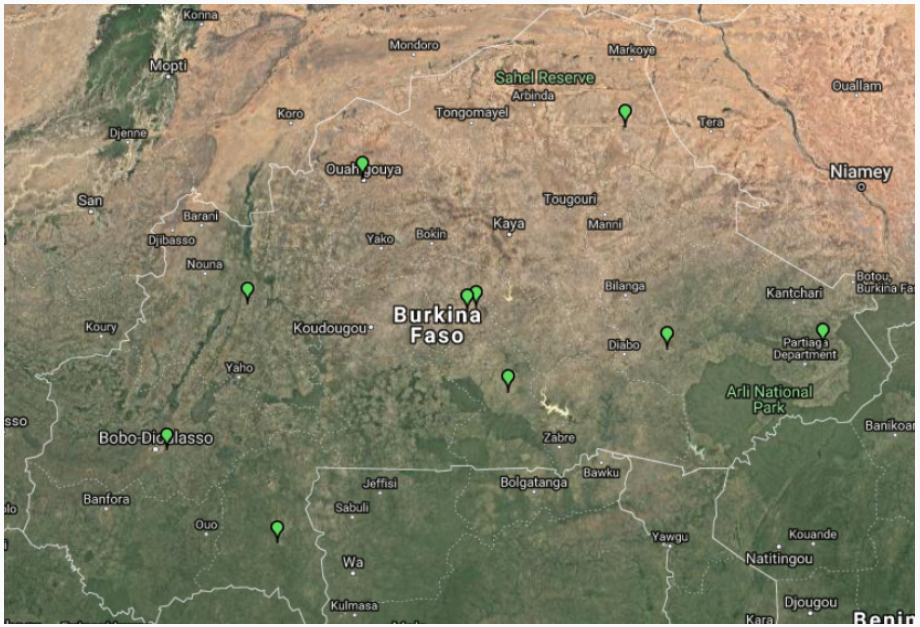

- This network is composed of 9 stations
- Data are stored under RINEX Format
- The data are accessible through an authorization
- The network is manage by the Institue Géographique du Burkina

The station network in Nigeria

- This network is composed of 15 stations
- Data are stored under RINEX Format
- The data are accessible through an authorization grant by NigNet
- The network is owned, maintained and operated by Presidential Technical Committee on Land Reform and the Office of the Surveyor General of Federation, as part of NigNet

Ionospheric Behavior over west Africa

Variation of S4 index

S4 variation recorded by the SCINDA station of Abidjan *(Ackah et al., 2011)*

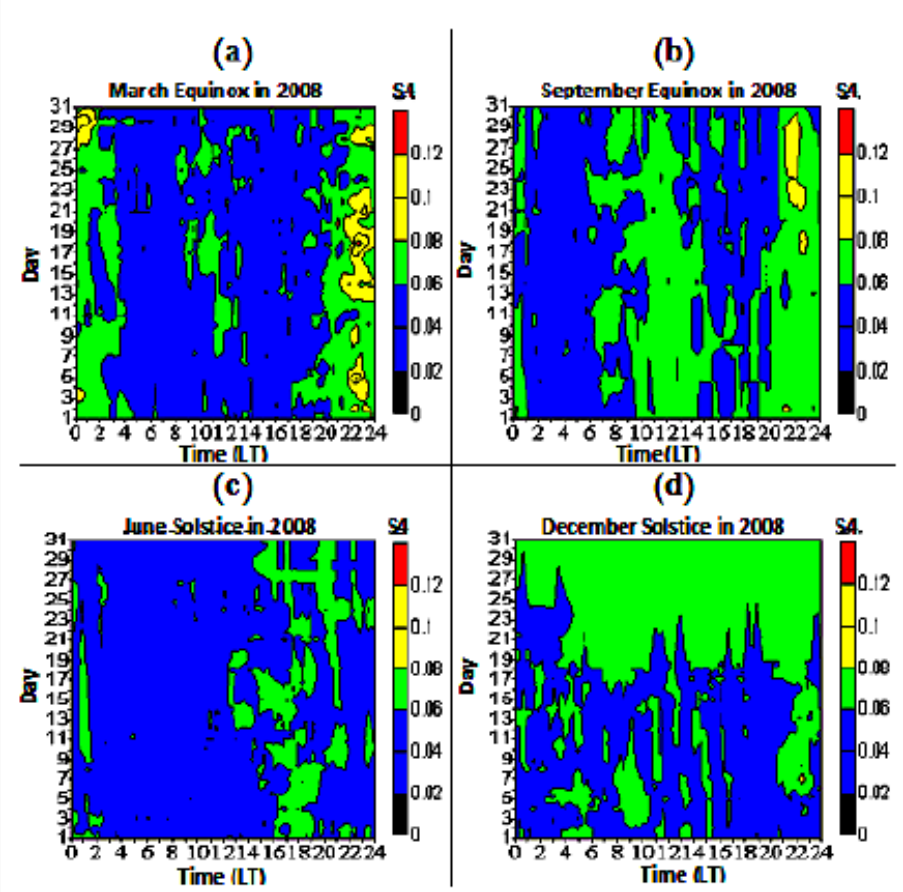

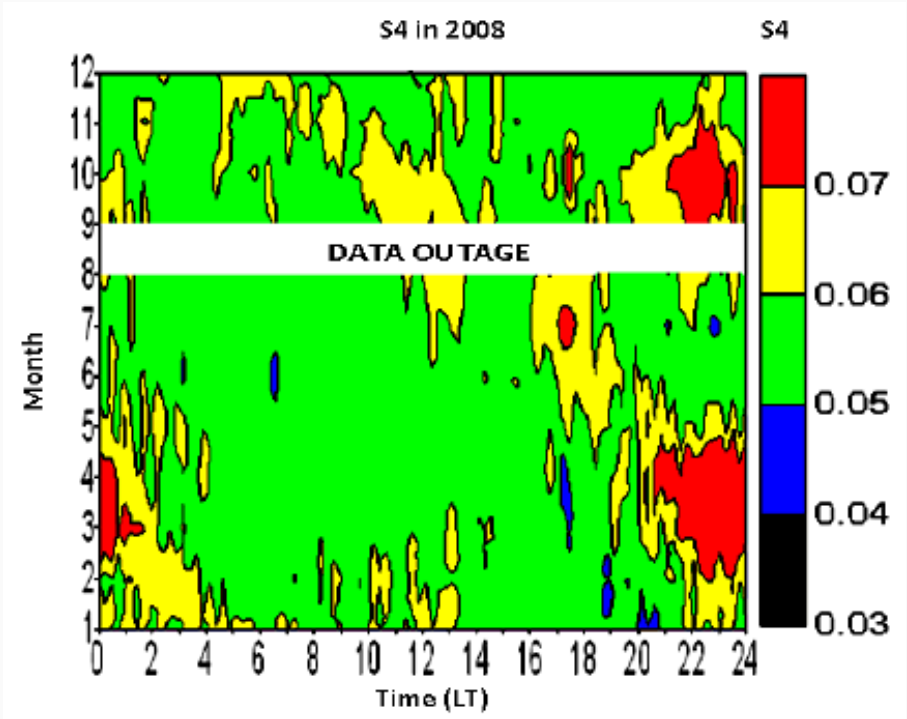

Safety of Air Navigation in Africa and Madagascar (ASECNA) and the Centre National d'Etudes Spatiales (CNES), have have signed a new agreement concerning the project to develop, deploy and commission ASECNA's Satellite Based Augmentation System (SBAS).

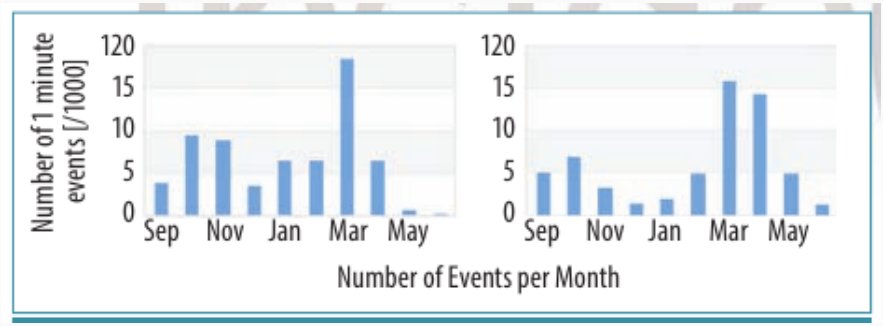

Figure 7: Number of events per month in Dakar (left panel) & Lomé (right) Secretan et al., (2014)

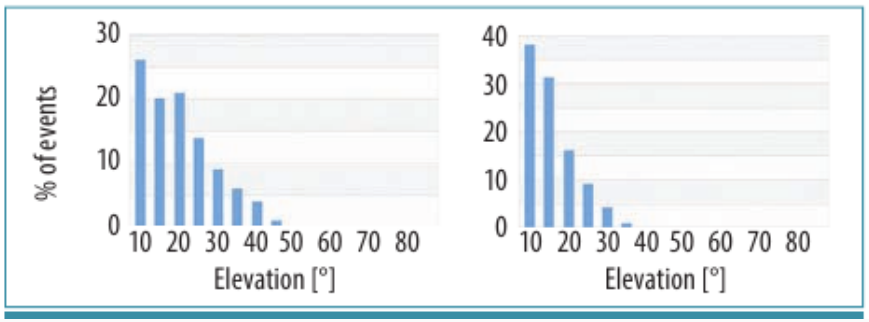

Figure 8: Repartition of the elevation of the LoS under scintillation in Dakar (left panel) & Lomé (right) Secretan et al., (2014)

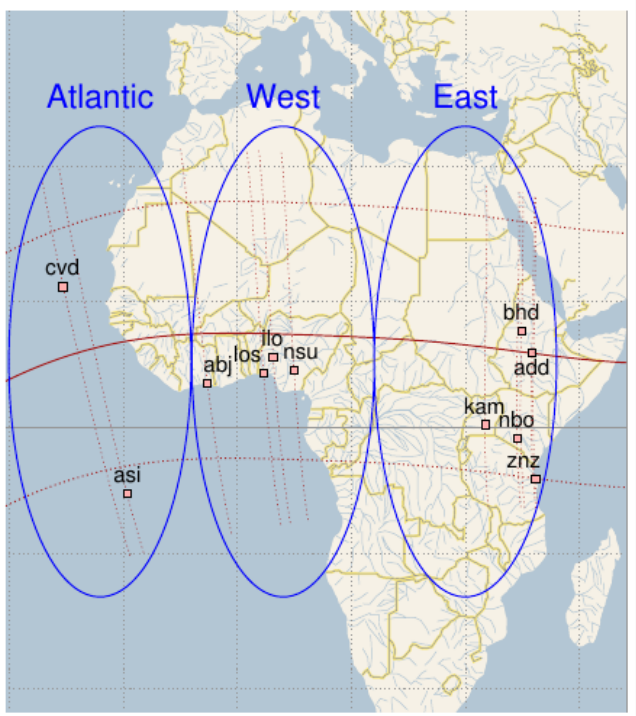

S4 index measurements as function of day of the season and universal time. for the year 2010 from three regions: Cape Verde, Lagos, and Kampala. Black color has been used to indicate missing data.(Paznukhov et al., 2012)

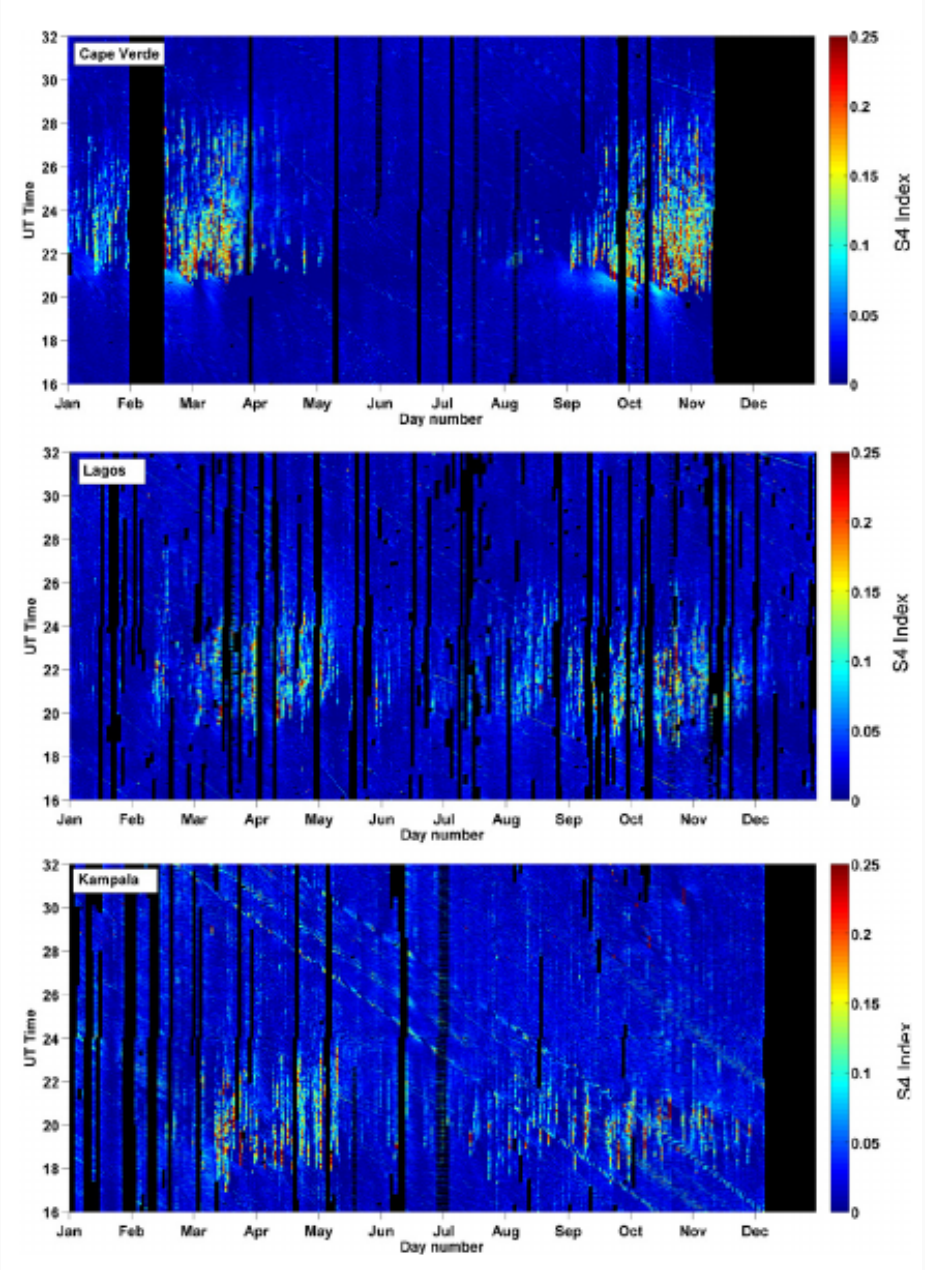

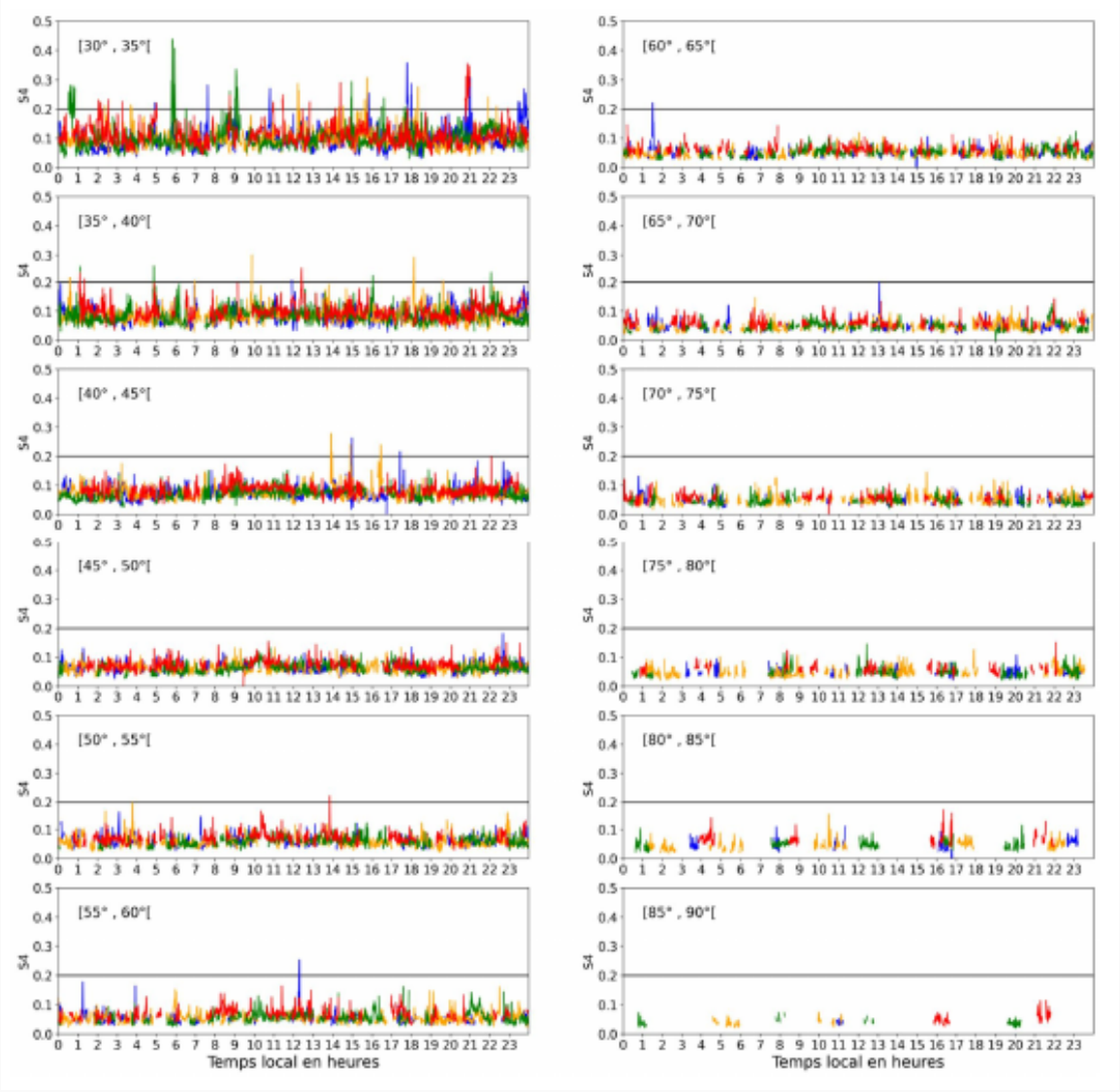

Variation of the S4 index with respect to the elevation angle over Korhogo (

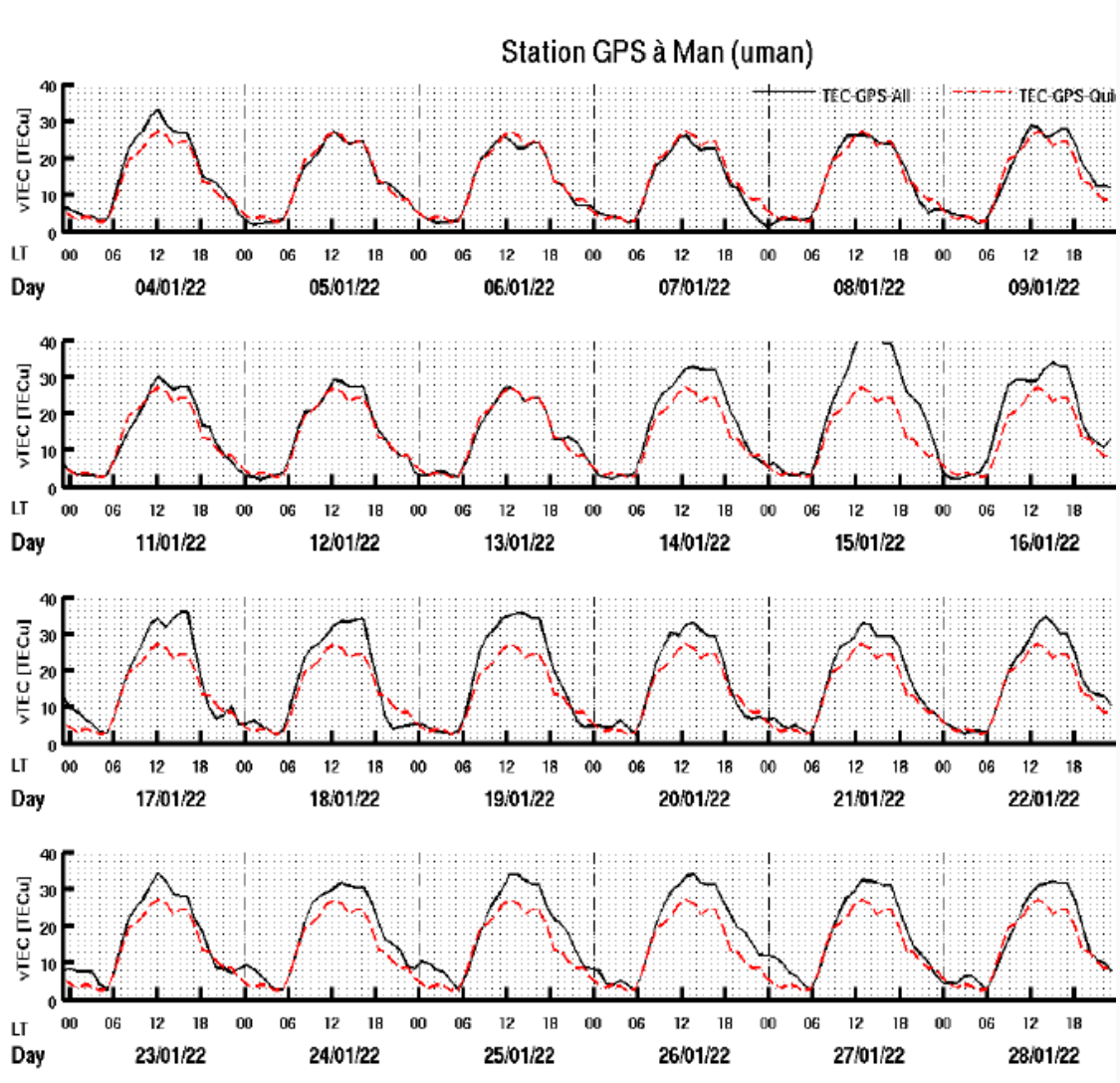

Figure 9: Diurnal variation of the TEC derived from GPS receiver insalled at the University of Man (Lat :7.40 Long ; -7.55) (TWAS Grant # 12-100 RG/PHY/AC-I)

Modeling of the ionosphere

AfriTEC Model

This work by Okoh et al., (2020) presents the development of a storm-time Total Electron Content (TEC) model over the African sector. It is based on artificial neural networks which are used to learn the relationship between TEC and the corresponding physical/geophysical input parameters representing factors which influence ionospheric variability.

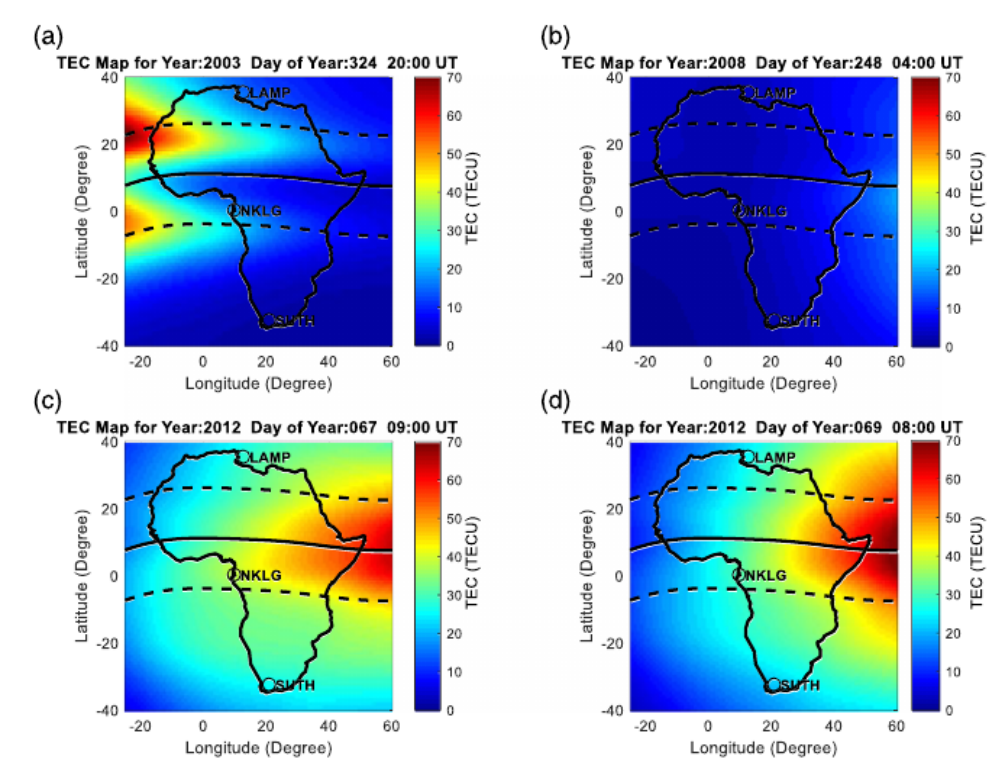

https://www.mathworks.com/matlabcentral/fileexchange/69257-african-gnss-tec-afritec-model

Validation of the NeQuick Model

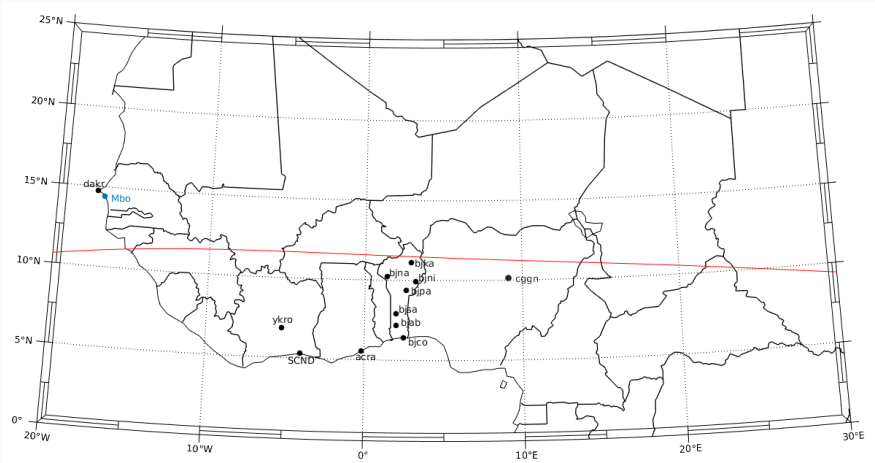

Figure 10: Map of the GPS stations

N°	Station Id	Location	Country	Geographic coordinates	
				Lat(°)	Long(°)
1	acra	Accra	Ghana	5.56N	0.203W
2	bjab	Abomey	Benin	7.18N	2.001E
3	bjco	Cotonou	Benin	6.39N	2.450E
4	bjka	Kandi	Benin	11.13N	2.928E
5	bjna	Natitingou	Benin	10.25N	1.381 E
6	bjni	Nikki	Benin	9.95N	3.204E
7	bjpa	Parakou	Benin	9.36N	2.626E
8	bjsa	Savalou	Benin	7.93N	1.993E
9	cggn	Toro	Nigéria	10.12N	9.118E
10	dakr	Dakar	Sénégal	14.72N	17.44W
11	Abja	Abidjan	Côte d'Ivoire	5.32N	4W
12	ykro	Yamoussou	Côte d'Ivoire	6.87N	5.24W

Figure 11: Coordinates of the stations

The TEC used in this current study are derived from GPS receivers data collected from the above station mainly localized in West Africa.

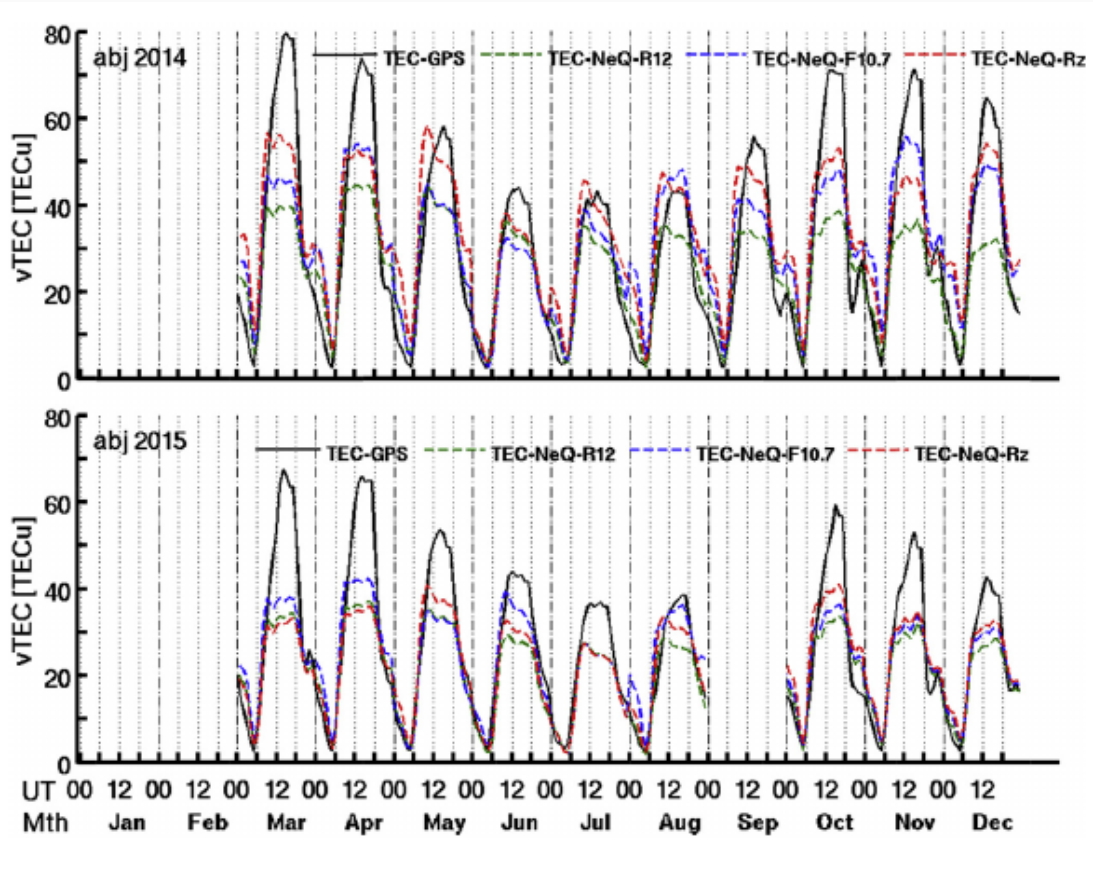

Monthly average of vertical TEC during the quiet days of the years 2014-2015 in abj station. TEC GPS in continuous black line (TEC-GPS), TEC NeQuick 2 driven by R12 (TEC- NeQ-R12) in dashed green line, TEC NeQuick 2 driven by Rz (TEC-NeQ-Rz) in dashed red line and TEC NeQuick 2 driven by F10.7 (TEC-NeQ-F10.7) in dashed blue line. The lack of data for monthly average is expressed by missing of the relevant lines. (Yao et al., 2018)

Space Weather effect on GNSS

Space Weather effect on GNSS

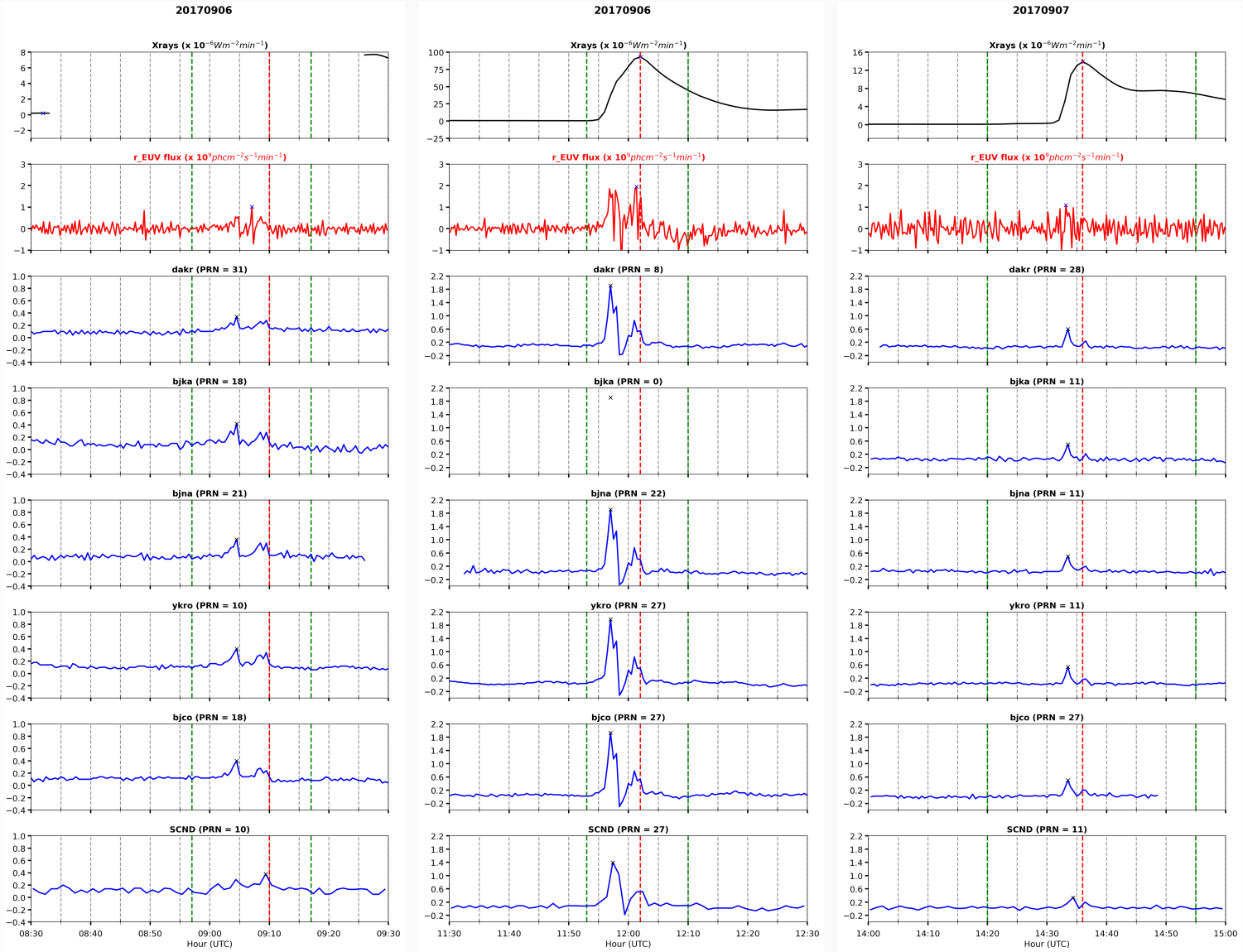

Figure 12: Variation of the time rate of change of TEC, X-ray and EUV

Thanks for your attention !